Supporting Information

Hirsutinolide series inhibit Stat3 activity, alter GCN1, MAP1B, Hsp105, G6PD, vimentin and importin α-2 expression, and induce antitumor effects against human glioma

Gabriella Miklossy[1,2], Ui Joung Youn[3], Peibin Yue[1,2], Mingming Zhang[3], Chih-Hong Chen[4], Tyvette S. Hilliard[1,2], David Paladino[1,2], Yifei Li[4], Justin Choi[4], Jann N. Sarkaria[5], Joel K. Kawakami[6], Supakit Wongwiwatthananukit[3], Yuan Chen[4], Dianqing Sun[3], Leng Chee Chang[3], and James Turkson[1,2,*]

[1]Natural Products and Experimental Therapeutics and [2]Cancer Biology Programs, University of Hawaii Cancer Center, University of Hawaii at Manoa, Honolulu, HI, [3]Department of Pharmaceutical Sciences, The Daniel K. Inouye College of Pharmacy, University of Hawaii at Hilo, Hilo, HI, [4]Department of Molecular Medicine, Beckman Research Institute of the City of Hope, Duarte, CA, [5]Department of Radiation Oncology, Mayo Clinic, Rochester, MN, [6]Division of Natural Sciences and Mathematics, Chaminade University, Honolulu, HI

Content:
Materials and Methods
Figures and Figure Legends

Keywords: Natural products, hirsutinolides, Stat3, glioma, xenografts, antitumor effects, GCN1, Vimentin and importin α-2, microtubule-associated protein 1B; thioredoxin reductase 1 cytoplasmic isoform 3; glucose-6-phosphate 1-dehydrogenase isoform a; heat shock protein105; and tumor necrosis factor α-induced protein 2.

Materials and Methods

All reagents and solvents were purchased from commercial sources and used without further purification.

Semi-synthesis of natural product analogs

We performed re-synthesis of **22** or the semi-synthesis of its analogs using **14**, **8**, or **17** as a starting material to expand the existing SAR of isolated natural hirsutinolides (Scheme 1). This was accomplished by reacting the isolated major natural product components, **14**, **8** or **17** with a selected panel of carboxylic acids in the presence of dicyclohexylcarbodiimide (DCC) and catalytic amounts of 4-(dimethylamino)pyridine (DMAP) by conventional Steglich esterification [1], affording the desired semi-synthetic derivatives in 40-85% yields. Due to the difficulty in removing the dicyclohexylurea byproduct and to further facilitate the purification process, Yamaguchi esterification protocol was employed to scale-up semi-synthesis of compound **22** [2]. Briefly, the Yamaguchi mixed anhydride was generated *in situ* from 2,4,6-trichlorobenzoyl chloride and tiglic acid [3], followed by the treatment with **14** in the presence of catalytic DMAP in toluene to afford **22** in 78% yield (Scheme 2). Title compounds were purified by normal phase column chromatography, preparative TLC, and/or semi-preparative reverse phase HPLC. The spectroscopic data of our semi-synthetic **22** are in full agreement with those of isolated natural products [4].

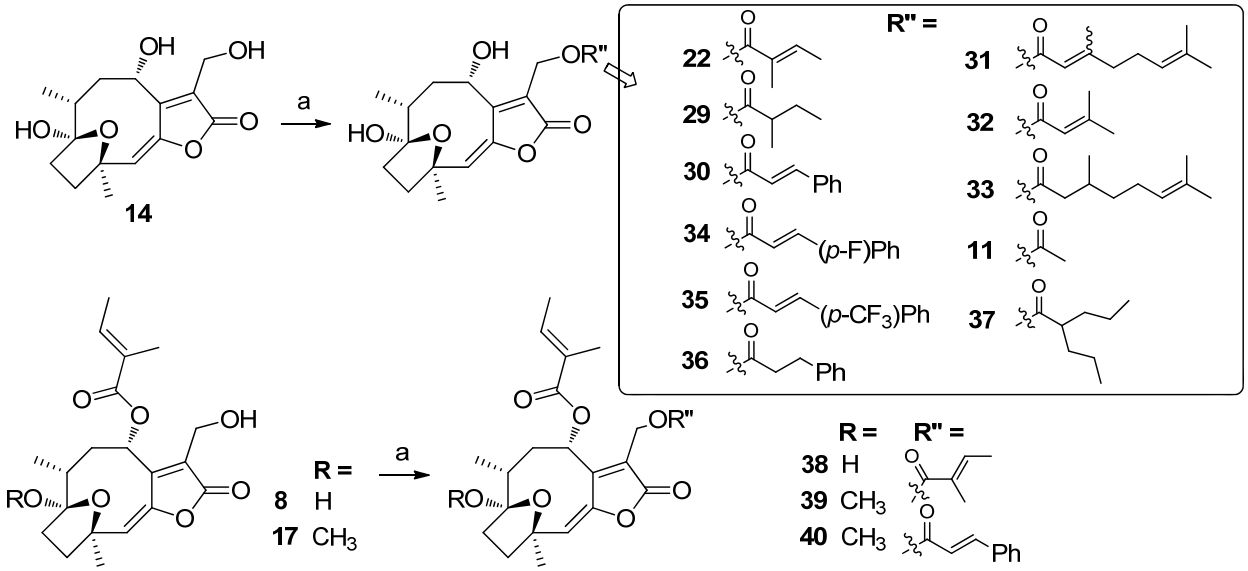

Scheme S1. Semi-synthesis of hirsutinolide derivatives. (a) Appropriate carboxylic acid (R"COOH), DCC, DMAP, CH_2Cl_2, room temperature (rt), 24 h, 40-85%.

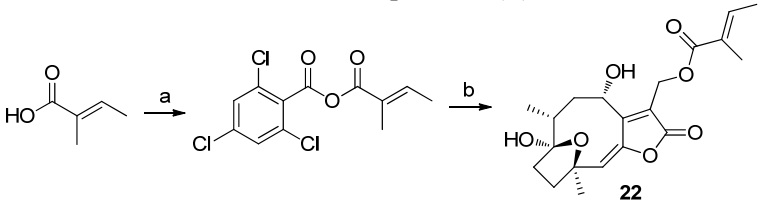

Scheme S2. Scale-up semi-synthesis of **22**. (a) 2,4,6-trichlorobenzoyl chloride, diisopropylethylamine (DIPEA), toluene, rt, 5 h, 32%. (b) **14**, DMAP, toluene, 50 ºC, 24 h, 78%.

General information

Solvents and reagents were purchased from Sigma-Aldrich and Fisher Scientific and were used without further purification. All reactions were monitored by either TLC or HPLC (Shimadzu LC-20A series system). Compounds were purified by flash column chromatography on silica gel using a Biotage Isolera One system, preparative silica gel TLC plate (w/UV254, glass backed, 500 μm, 20 × 20 cm; Sorbent Technologies), and/or semi-preparative reverse phase HPLC. Proton nuclear magnetic resonance (^{1}H NMR) spectra were recorded employing a Bruker AVANCE (400 MHz) spectrometer. Chemical shifts were expressed in parts per million (ppm), *J* values were in Hertz. Mass spectra were recorded on a Varian 500-MS IT mass spectrometer using ESI. The purity of compounds was determined by analytical HPLC (Shimadzu LC-20A series) using a Gemini, 3 μM, C18, 110 Å column (50 mm × 4.6 mm, Phenomenex) and flow rate of 1 mL/min. Gradient conditions: solvent A (0.1% trifluoroacetic acid in water) and solvent B (acetonitrile): 0-2.0 min 100% A, 2.0-7.0 min 0-100% B (linear gradient), 7.0-8.0 min 100% B. UV detection at 254 nm and 284 nm. All the tested compounds were obtained with ≥ 96.0% purity by HPLC.

General procedure for the semi-synthesis of hirsutinolide derivatives

To a stirred solution of **14, 8,** or **17** (0.0068 mmol) in anhydrous CH_2Cl_2 (2 mL) was added DMAP (0.42 mg, 0.0034 mmol) and appropriate carboxylic acid (0.0136 mmol). DCC (2.81 mg, 0.0136 mmol) was added to the reaction at 0 ºC and the reaction mixture was then stirred for 5 min at 0 ºC and 24 h at room temperature. The residue was purified by preparative TLC (Hexane-Ethyl Acetate as developing solvent) and/or semi-preparative reverse phase HPLC to give desired target compounds in 40-85% yields.

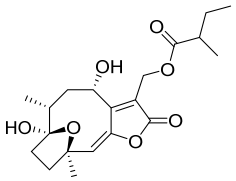

(29) ((4*S*,6*R*,*E*)-4,7-dihydroxy-6,10-dimethyl-2-oxo-2,4,5,6,7,8,9,10-octahydro-7,10-epoxycyclodeca[*b*]furan-3-yl)methyl 2-methylbutanoate. White amorphous powder (2.17 mg, 84%); ^{1}H NMR (400 MHz, $CDCl_3$) δ 6.15 (d, *J* = 11.5 Hz, 1H), 5.88 (s, 1H), 5.17 (dd, *J* = 12.4, 6.1 Hz, 1H), 4.98 – 4.86 (m, 2H), 2.52 (s, 1H), 2.45 – 2.39 (m, 1H), 2.36 (d, *J* = 7.7 Hz, 1H), 2.31 – 2.21 (m, 3H), 2.11 – 2.07 (m, 1H), 1.87 (dd, *J* = 15.8, 7.0 Hz, 2H), 1.69 (s, 2H), 1.63 (s, 3H), 1.17 (dd, *J* = 7.0, 1.2 Hz, 3H), 0.99 (d, *J* = 6.9 Hz, 3H), 0.93 (t, *J* = 8.0 Hz, 3H). LRMS (ES+) calculated for [$C_{20}H_{28}O_7$ + Na] 403.2, found 403.4. HPLC purity: 99.2% (254 nm), t_R: 6.54 min, 99.2% (284 nm), t_R: 6.54 min.

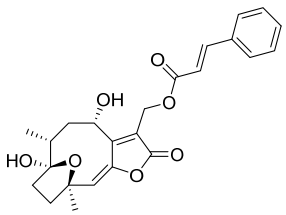

(30) ((4*S*,6*R*,*E*)-4,7-dihydroxy-6,10-dimethyl-2-oxo-2,4,5,6,7,8,9,10-octahydro-7,10-epoxycyclodeca[*b*]furan-3-yl)methyl cinnamate. White amorphous powder (2.46 mg, 85%); ^{1}H NMR (400 MHz, $CDCl_3$) δ 7.74 (d, *J* = 16.0 Hz, 1H), 7.53 (dd, *J* = 6.8, 2.9 Hz, 2H), 7.46 – 7.36 (m, 3H), 6.44 (d, *J* = 16.0 Hz, 1H), 6.19 (d, *J* = 11.8 Hz, 1H), 5.89 (s, 1H), 5.30 – 5.19 (m,

1H), 5.06 (s, 2H), 2.65 (s, 1H), 2.32 – 2.16 (m, 4H), 2.11 – 2.03 (m, 1H), 1.95 (dd, *J* = 12.1, 6.9 Hz, 1H), 1.92 – 1.84 (m, 1H), 1.63 (s, 3H), 0.97 (d, *J* = 6.8 Hz, 3H). LRMS (ES+) calculated for [$C_{24}H_{26}O_7$ + Na] 449.2, found 449.1. HPLC purity: 97.1% (254 nm), t_R: 6.72 min, 97.7% (284 nm), t_R: 6.54 min.

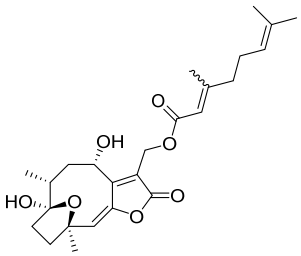

(31) ((4*S*,6*R*,*E*)-4,7-dihydroxy-6,10-dimethyl-2-oxo-2,4,5,6,7,8,9,10-octahydro-7,10-epoxycyclodeca[*b*]furan-3-yl)methyl 3,7-dimethylocta-2,6-dienoate. White amorphous powder (1.37 mg, 45%); ^{1}H NMR (400 MHz, $CDCl_3$) δ 6.16 (t, *J* = 12.1 Hz, 1H), 5.87 (d, *J* = 11.0 Hz, 1H), 5.24 – 5.04 (m, 2H), 4.98 – 4.87 (m, 2H), 2.31 – 2.05 (m, 10H), 2.00 – 1.92 (m, 2H), 1.92 – 1.82 (m, 2H), 1.70 (s, 3H), 1.63 (d, *J* = 6.8 Hz, 6H), 0.98 (t, *J* = 7.3 Hz, 3H). LRMS (ES+) calculated for [$C_{25}H_{34}O_7$ + Na] 469.2, found 469.5. HPLC purity: 99.8% (254 nm), t_R: 7.21 min, 99.9% (284 nm), t_R: 7.21 min.

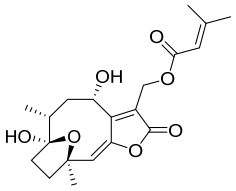

(32) ((4*S*,6*R*,*E*)-4,7-dihydroxy-6,10-dimethyl-2-oxo-2,4,5,6,7,8,9,10-octahydro-7,10-epoxycyclodeca[*b*]furan-3-yl)methyl 3-methylbut-2-enoate. White amorphous powder (1.26 mg, 49%); ^{1}H NMR (400 MHz, $CDCl_3$) δ 6.14 (d, *J* = 11.8 Hz, 1H), 5.86 (s, 1H), 5.70 – 5.64 (m, 1H), 5.24 – 5.16 (m, 1H), 4.98 – 4.88 (m, 2H), 2.60 (s, 1H), 2.30 – 2.11 (m, 6H), 2.11 – 2.04 (m, 1H), 2.01 – 1.79 (m, 6H), 1.62 (s, 3H), 0.97 (d, *J* = 6.8 Hz, 3H). LRMS (ES+) calculated for [$C_{20}H_{26}O_7$ + Na] 401.2, found 401.4. HPLC purity: 97.9% (254 nm), t_R: 6.43 min, 99.4% (284 nm), t_R: 6.43 min.

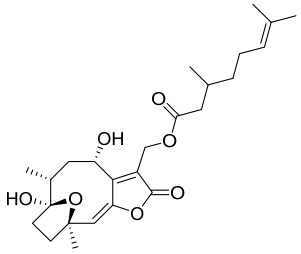

(33) ((4*S*,6*R*,*E*)-4,7-dihydroxy-6,10-dimethyl-2-oxo-2,4,5,6,7,8,9,10-octahydro-7,10-epoxycyclodeca[*b*]furan-3-yl)methyl 3,7-dimethyloct-6-enoate. White amorphous powder (2.34 mg, 77%); ^{1}H NMR (400 MHz, $CDCl_3$) δ 6.17 (d, *J* = 11.6 Hz, 1H), 5.88 (s, 1H), 5.24 – 5.12 (m, 1H), 5.09 (dd, *J* = 7.7, 6.4 Hz, 1H), 4.97 – 4.85 (m, 2H), 2.65 (s, 1H), 2.41 – 1.80 (m, 13H), 1.70 (d, *J* = 1.0 Hz, 4H), 1.62 (s, 3H), 1.61 (s, 4H), 0.99 (d, *J* = 6.8 Hz, 3H), 0.96 (d, *J* = 6.6 Hz, 3H). LRMS (ES+) calculated for [$C_{25}H_{36}O_7$ + Na] 471.2, found 471.4. HPLC purity: 98.9% (254 nm), t_R: 7.26 min, 98.8% (284 nm), t_R: 7.26 min.

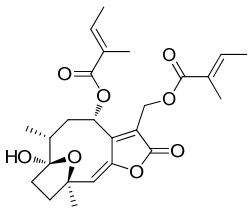

(38) (4*S*,6*R*,*E*)-7-hydroxy-6,10-dimethyl-3-((((*E*)-2-methylbut-2-enoyl)oxy)methyl)-2-oxo-2,4,5,6,7,8,9,10-octahydro-7,10-epoxycyclodeca[*b*]furan-4-yl (*E*)-2-methylbut-2-enoate. White amorphous powder (1.25 mg, 40%); ^{1}H NMR (400 MHz, CD_3OD) δ 7.13 (dd, *J* = 7.1, 1.5 Hz, 1H), 6.93 (dd, *J* = 7.0, 1.4 Hz, 1H), 6.28 (d, *J* = 7.6 Hz, 1H), 6.04 (s, 1H), 5.14 (d, *J* = 13.0 Hz, 1H), 5.01 (d, *J* = 12.9 Hz, 1H), 2.40 (dd, *J* = 16.2, 12.2 Hz, 1H), 2.12 (dd, *J* = 11.5, 5.6 Hz, 2H), 1.92 – 1.84 (m, 9H), 1.84 – 1.79 (m, 6H), 1.75 (s, 1H), 1.49 (s, 3H), 0.88 (d, *J* = 6.9 Hz, 3H). LRMS (ES+) calculated for [$C_{25}H_{32}O_8$ + Na] 483.2, found 483.4. HPLC purity: 99.7% (254 nm), t_R: 7.14 min, 99.7% (284 nm), t_R: 7.14 min.

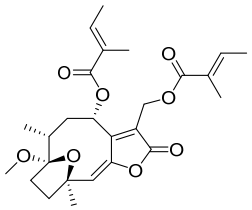

***(39) (4S,6R,E)*-7-methoxy-6,10-dimethyl-3-((((*E*)-2-methylbut-2-enoyl)oxy)methyl)-2-oxo-2,4,5,6,7,8,9,10-octahydro-7,10-epoxycyclodeca[*b*]furan-4-yl (*E*)-2-methylbut-2-enoate.** White amorphous powder (1.35 mg, 42%); ^{1}H NMR (400 MHz, $CDCl_3$) δ 7.05 (dd, *J* = 7.1, 1.5 Hz, 1H), 6.95 – 6.84 (m, 1H), 6.27 (d, *J* = 7.6 Hz, 1H), 5.87 (s, 1H), 5.20 (d, *J* = 13.1 Hz, 1H), 5.07 (d, *J* = 12.9 Hz, 1H), 3.29 (s, 3H), 2.38 (dd, *J* = 15.6, 11.9 Hz, 1H), 2.23 – 2.07 (m, 2H), 2.02 – 1.86 (m, 3H), 1.84 (dt, *J* = 2.6, 1.3 Hz, 6H), 1.80 (dd, *J* = 7.1, 1.1 Hz, 6H), 1.76 (d, *J* = 10.0 Hz, 1H), 1.51 (s, 3H), 0.86 (d, *J* = 7.0 Hz, 3H). LRMS (ES+) calculated for [$C_{26}H_{34}O_8$ + Na] 497.2, found 497.5. HPLC purity: 99.8% (254 nm), t_R: 7.76 min, 99.8% (284 nm), t_R: 7.76 min.

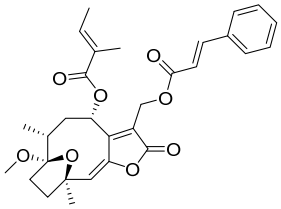

(40) (4*S*,6*R*,*E*)-3-((cinnamoyloxy)methyl)-7-methoxy-6,10-dimethyl-2-oxo-2,4,5,6,7,8,9,10-octahydro-7,10-epoxycyclodeca[*b*]furan-4-yl (*E*)-2-methylbut-2-enoate. White amorphous powder (2.91 mg, 82%); ^{1}H NMR (400 MHz, $CDCl_3$) δ 7.73 (d, *J* = 16.0 Hz, 1H), 7.53 (dd, *J* = 6.7, 2.9 Hz, 2H), 7.45 – 7.37 (m, 3H), 7.06 (dd, *J* = 7.1, 1.5 Hz, 1H), 6.43 (d, *J* = 16.0 Hz, 1H), 6.34 (d, *J* = 7.8 Hz, 1H), 5.90 (s, 1H), 5.30 (d, *J* = 13.0 Hz, 1H), 5.14 (d, *J* = 12.9 Hz, 1H), 3.29 (s, 3H), 2.41 (dd, *J* = 15.8, 11.3 Hz, 1H), 2.23 – 2.06 (m, 2H), 1.95 (ddd, *J* = 16.9, 15.8, 9.5 Hz, 3H), 1.85 (dd, *J* = 5.8, 4.5 Hz, 4H), 1.80 (dd, *J* = 7.1, 1.1 Hz, 3H), 1.51 (s, 3H), 0.87 (d, *J* = 6.9 Hz, 3H). LRMS (ES+) calculated for [$C_{30}H_{34}O_8$ + Na] 545.2, found 545.2. HPLC purity: 96.0% (254 nm), t_R: 7.88 min, 97.5% (284 nm), t_R: 7.88 min.

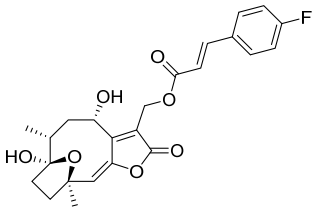

(34) ((4*S*,6*R*,*E*)-4,7-dihydroxy-6,10-dimethyl-2-oxo-2,4,5,6,7,8,9,10-octahydro-7,10-epoxycyclodeca[*b*]furan-3-yl)methyl (*E*)-3-(4-fluorophenyl)acrylate. White amorphous powder (1.6 mg, 53%); ^{1}H NMR (400 MHz, $CDCl_3$) δ 7.69 (d, *J* = 16.0 Hz, 1H), 7.58 – 7.46 (m, 2H), 7.10 (t, *J* = 8.6 Hz, 2H), 6.36 (d, *J* = 16.0 Hz, 1H), 6.17 (d, *J* = 11.8 Hz, 1H), 5.90 (s, 1H), 5.29 – 5.20 (m, 1H), 5.05 (s, 2H), 2.59 (s, 1H), 2.33 – 2.16 (m, 4H), 2.11 – 2.03 (m, 1H), 1.95 (dd, *J* = 12.1, 6.8 Hz, 1H), 1.91 – 1.83 (m, 1H), 1.63 (s, 3H), 0.97 (d, *J* = 6.8 Hz, 3H). LRMS (ES+) calculated for [$C_{24}H_{25}FO_7$ + Na] 467.1, found 467.1. HPLC purity: 96.4% (254 nm), t_R: 6.77 min, 97.2% (284 nm), t_R: 6.77 min.

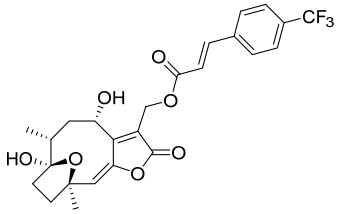

(35) ((4*S*,6*R*,*E*)-4,7-dihydroxy-6,10-dimethyl-2-oxo-2,4,5,6,7,8,9,10-octahydro-7,10-epoxycyclodeca[*b*]furan-3-yl)methyl (*E*)-3-(4-(trifluoromethyl)phenyl)acrylate. White amorphous powder (1.6 mg, 48%); ^{1}H NMR (400 MHz, $CDCl_3$) δ 7.74 (d, *J* = 16.0 Hz, 1H), 7.65 (q, *J* = 8.5 Hz, 4H), 6.51 (d, *J* = 16.0 Hz, 1H), 6.19 (d, *J* = 11.8 Hz, 1H), 5.91 (s, 1H), 5.25 (dd, *J* = 11.8, 5.4 Hz, 1H), 5.07 (s, 2H), 2.58 (s, 1H), 2.34 – 2.15 (m, 4H), 2.13 – 2.03 (m, 1H), 1.96 (dd, *J* = 13.3, 5.9 Hz, 1H), 1.92 – 1.82 (m, 1H), 1.63 (s, 3H), 0.98 (d, *J* = 6.8 Hz, 3H). LRMS (ES+) calculated for [$C_{25}H_{25}F_3O_7$ + Na] 517.1, found 517.1. HPLC purity: 96.3% (254 nm), t_R: 7.04 min, 96.3% (284 nm), t_R: 7.04 min.

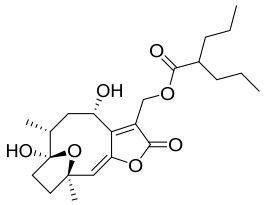

(37) ((4*S*,6*R*,*E*)-4,7-dihydroxy-6,10-dimethyl-2-oxo-2,4,5,6,7,8,9,10-octahydro-7,10-epoxycyclodeca[*b*]furan-3-yl)methyl 2-propylpentanoate. White amorphous powder (1.4 mg, 49%); ^{1}H NMR (400 MHz, $CDCl_3$) δ 6.16 (d, *J* = 11.8 Hz, 1H), 5.89 (s, 1H), 5.21 – 5.12 (m, 1H), 4.91 (dd, *J* = 30.8, 12.9 Hz, 2H), 2.58 (s, 1H), 2.45 – 2.34 (m, 1H), 2.24 (ddd, *J* = 15.7, 13.0, 10.7 Hz, 3H), 2.11 – 2.03 (m, 1H), 1.92 (ddd, *J* = 15.7, 9.4, 5.5 Hz, 2H), 1.63 (s, 3H), 1.44 (dddd, *J* = 10.5, 7.7, 6.6, 4.0 Hz, 2H), 1.36 – 1.23 (m, 6H), 1.00 (d, *J* = 6.8 Hz, 2H), 0.91 (td, *J* = 7.3, 1.2 Hz, 6H). LRMS (ES+) calculated for [$C_{23}H_{34}O_7$ + Na] 445.2, found 445.1. HPLC purity: 99.0% (254 nm), t_R: 7.09 min, 99.0% (284 nm), t_R: 7.09 min.

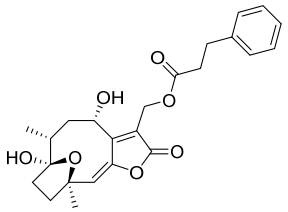

(36) ((4*S*,6*R*,*E*)-4,7-dihydroxy-6,10-dimethyl-2-oxo-2,4,5,6,7,8,9,10-octahydro-7,10-epoxycyclodeca[*b*]furan-3-yl)methyl 3-phenylpropanoate. White amorphous powder (2.0 mg, 69%); ^{1}H NMR (400 MHz, $CDCl_3$) δ 7.34 – 7.17 (m, 5H), 6.15 (d, *J* = 11.8 Hz, 1H), 5.88 (s, 1H), 5.17 – 5.08 (m, 1H), 4.91 (s, 2H), 2.97 (t, *J* = 7.7 Hz, 2H), 2.66 (dd, *J* = 8.4, 7.2 Hz, 2H), 2.57 (s, 1H), 2.28 – 2.15 (m, 4H), 2.10 – 2.02 (m, 1H), 1.90 (dd, *J* = 10.9, 5.8 Hz, 1H), 1.78 (ddd, *J* = 15.9, 6.9, 2.4 Hz, 1H), 1.62 (s, 3H), 0.96 (d, *J* = 6.8 Hz, 3H). LRMS (ES+) calculated for [$C_{24}H_{28}O_7$ + Na] 451.2, found 451.1. HPLC purity: 98.9% (254 nm), t_R: 6.68 min, 98.9% (284 nm), t_R: 6.68 min.

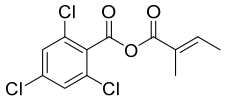

(*E*)-2,4,6-trichlorobenzoic (*E*)-2-methylbut-2-enoic anhydride. To a premixed solution of tiglic acid (300 mg, 3.0 mmol) and diisopropylethylamine (DIPEA, 0.62 mL, 3.6 mmol) in CH_2Cl_2 (15 mL) was added 2,4,6-trichlorobenzoyl chloride (0.61 mL, 3.6 mmol) dropwise at 0 ^{o}C. The resulting solution was stirred at room temperature for 5 h. Dry ether (20 mL) was then added to precipitate DIPEA hydrochloride, followed by the filtration. The filtrate solution was concentrated and the residue was purified by flash column chromatography (1 : 3, CH_2Cl_2 : hexanes) to afford the mixed anhydride as a white crystalline solid (293 mg, 32%). ^{1}H NMR (400 MHz, $CDCl_3$) δ 7.43 – 7.36 (m, 2H), 7.17 – 7.10 (m, 1H), 1.91 (dd, *J* = 2.2, 0.9 Hz, 3H), 1.91 – 1.88 (m, 3H). HPLC purity: 98.4% (254 nm), t_R: 7.55 min, 98.7% (284 nm), t_R: 7.55 min.

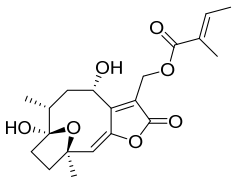

(22) ((4*S*,6*R*,*E*)-4,7-dihydroxy-6,10-dimethyl-2-oxo-2,4,5,6,7,8,9,10-octahydro-7,10-epoxycyclodeca[*b*]furan-3-yl)methyl (*E*)-2-methylbut-2-enoate. To a solution of **14** (18 mg, 0.061 mmol) in toluene (2 mL) was added DMAP (3.7 mg, 0.035 mmol) at room temperature. A solution of (*E*)-2,4,6-trichlorobenzoic (*E*)-2-methylbut-2-enoic anhydride (37.3 mg, 0.122 mmol) in toluene (1 mL) was next added, the reaction was heated at 80 ºC for 24 h. After cooling to room temperature, the reaction mixture was concentrated under reduced pressure and purified by flash column chromatography on silica gel (1: 5 to 1 : 2, ethyl acetate : hexanes), affording the title compound **22** as a white solid (19.6 mg, 85%). ^{1}H NMR (400 MHz, $CDCl_3$) δ 6.89 (qd, *J* = 7.0, 1.4 Hz, 1H), 6.15 (d, *J* = 11.8 Hz, 1H), 5.87 (s, 1H), 5.19 (ddd, *J* = 11.8, 6.8, 1.4 Hz, 1H), 4.97 (s, 2H), 2.25 (dd, *J* = 9.1, 6.7 Hz, 1H), 2.20 (d, *J* = 3.0 Hz, 1H), 2.18 (t, *J* = 5.0 Hz, 1H), 2.10 – 2.05 (m, 1H), 1.97 – 1.89 (m, 1H), 1.89 – 1.85 (m, 1H), 1.86 – 1.83 (m, 3H), 1.81 (dd, *J* = 7.1, 1.1 Hz, 3H), 1.62 (s, 3H), 0.96 (d, *J* = 6.8 Hz, 3H). LRMS (ES+) calculated for [$C_{20}H_{26}O_7$ + Na] 401.2, found 401.4. HPLC purity: 99.4% (254 nm), t_R: 6.42 min, 99.2% (284 nm), t_R: 6.42 min.

References

1. Neises B, Steglich W: Simple method for the esterification of carboxylic acids. *Angew Chem Int Ed Engl* **1978**, 17:522-524

2. Inanaga J, Hirata K, Saeki H, Katsuki T, Yamaguchi M: A rapid esterification by means of mixed anhydride and its application to large-ring lactonization. *Bull Chem Soc Jpn* **1979**, 52:1989-1993

3. Ball M, Andrews SP, Wierschem F, Cleator E, Smith MD, Ley SV: Total synthesis of thapsigargin, a potent SERCA pump inhibitor. *Org Lett* **2007**, 9:663-666

4. Youn UJ, Miklossy G, Chai X, Wongwiwatthananukit S, Toyama O, Songsak T, Turkson J, Chang LC: Bioactive sesquiterpene lactones and other compounds isolated from Vernonia cinerea. *Fitoterapia* **2014**, 93:194-200

Supplementary Figures

Fig. S1

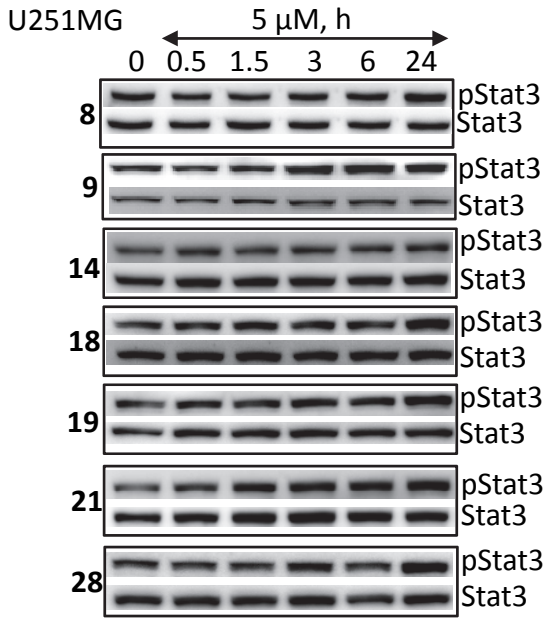

Figure S1. **Hirsutinolides inhibit Stat3 activation in tumor cells.** U251MG cells in culture were treated with 5 μM **8, 14**, **18**, **19, 21** or **28**, and whole-cell lysates of equal total protein prepared and subjected to immunoblotting analysis for pY705Stat3 and Stat3. Positions of proteins in gel are labeled; control lane (0) represents whole-cell lysates prepared from cells treated with 0.025% DMSO. Data are representative of 2-3 independent determinations.

Fig. S2.

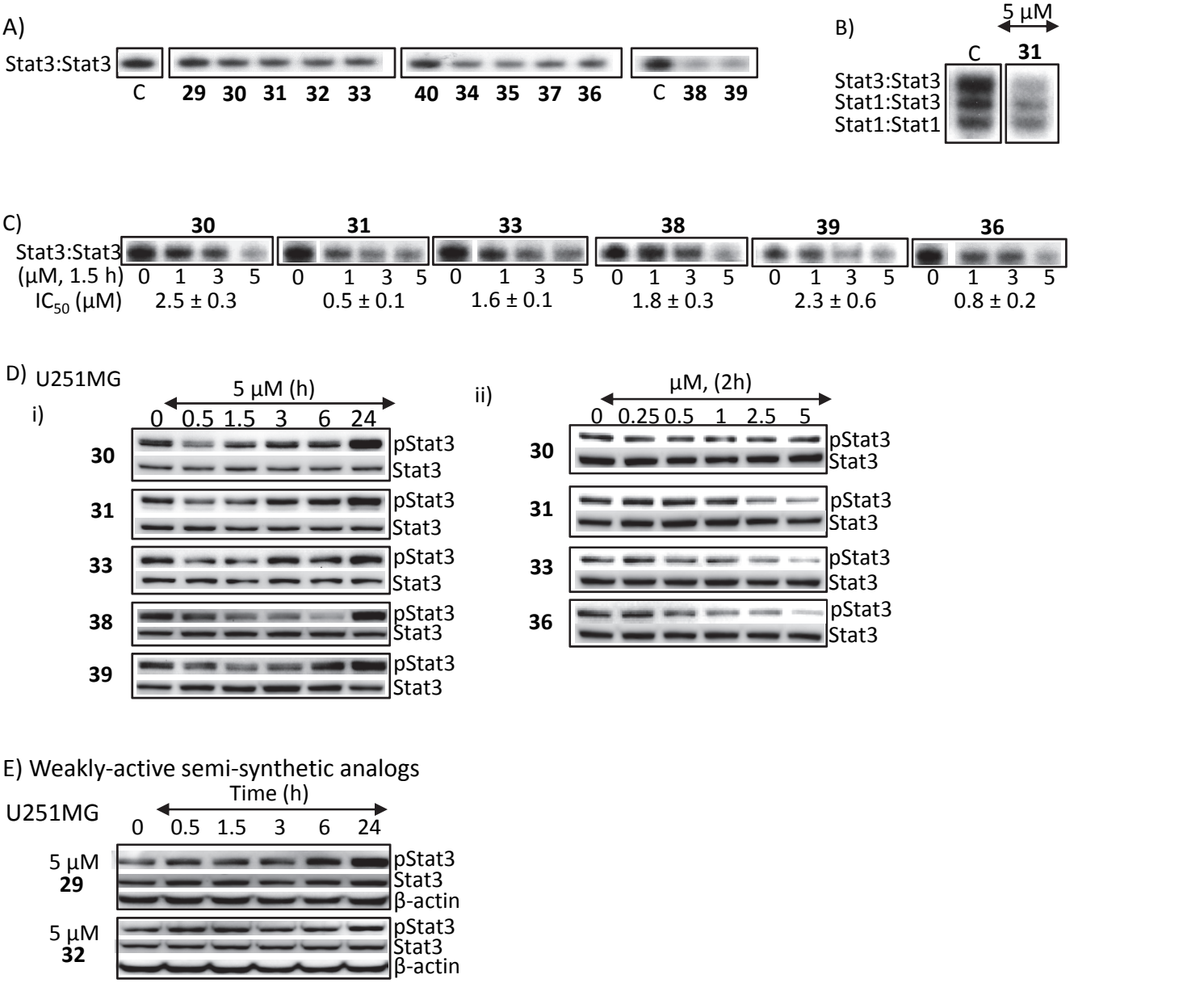
A)
Stat3:Stat3
C 29 30 31 32 33 40 34 35 37 36 C 38 39
B)
5 μM
C 31
Stat3:Stat3
Stat1:Stat3
Stat1:Stat1
C)
30 31 33 38 39 36
Stat3:Stat3
(μM, 1.5 h) 0 1 3 5 0 1 3 5 0 1 3 5 0 1 3 5 0 1 3 5 0 1 3 5
IC50 (μM) 2.5 ± 0.3 0.5 ± 0.1 1.6 ± 0.1 1.8 ± 0.3 2.3 ± 0.6 0.8 ± 0.2
D) U251MG
i)
5 μM (h)
0 0.5 1.5 3 6 24
30 31 33 38 39
pStat3
Stat3
ii)
μM, (2h)
0 0.25 0.5 1 2.5 5
30 31 33 36
pStat3
Stat3
E) Weakly-active semi-synthetic analogs
U251MG
Time (h)
0 0.5 1.5 3 6 24
5 μM 29
5 μM 32
pStat3
Stat3
β-actin

Figure S2. **Semi-synthetic analogs inhibit Stat3 activation.** (A-C) Nuclear extracts containing activated (A and B) Stat3 from NIH3T3/v-Src fibroblasts or (C) Stat1 and Stat3 from EGF-stimulated NIH3T3/hEGFR were pre-incubated with the designated semi-synthetic analogs for 30 min at room temperature prior to incubating with the radiolabeled hSIE probe that binds Stat1 and Stat3 and performing EMSA analysis; (D and E) Immunoblotting analysis of whole-cell lysates prepared from U251MG cells treated with the designated compounds at (D(i) and E) 5 μM for 0-24 h or (D(ii)) 0-5 μM for 2 h and probing for pStat3, Stat3 or β-actin. Positions of proteins or Stats:DNA complex in gel are labeled; control lane (c, 0) represents whole-cell lysates or nuclear extracts prepared from 0.025% DMSO-treated cells or nuclear extracts pre-treated with 0.025% DMSO. Bands corresponding to Stats:DNA complexes were scanned and quantified using ImageJ, plotted against concentration of agent from which IC_{50} values were derived. Data are representative of 2-3 independent determinations.

Fig. S3

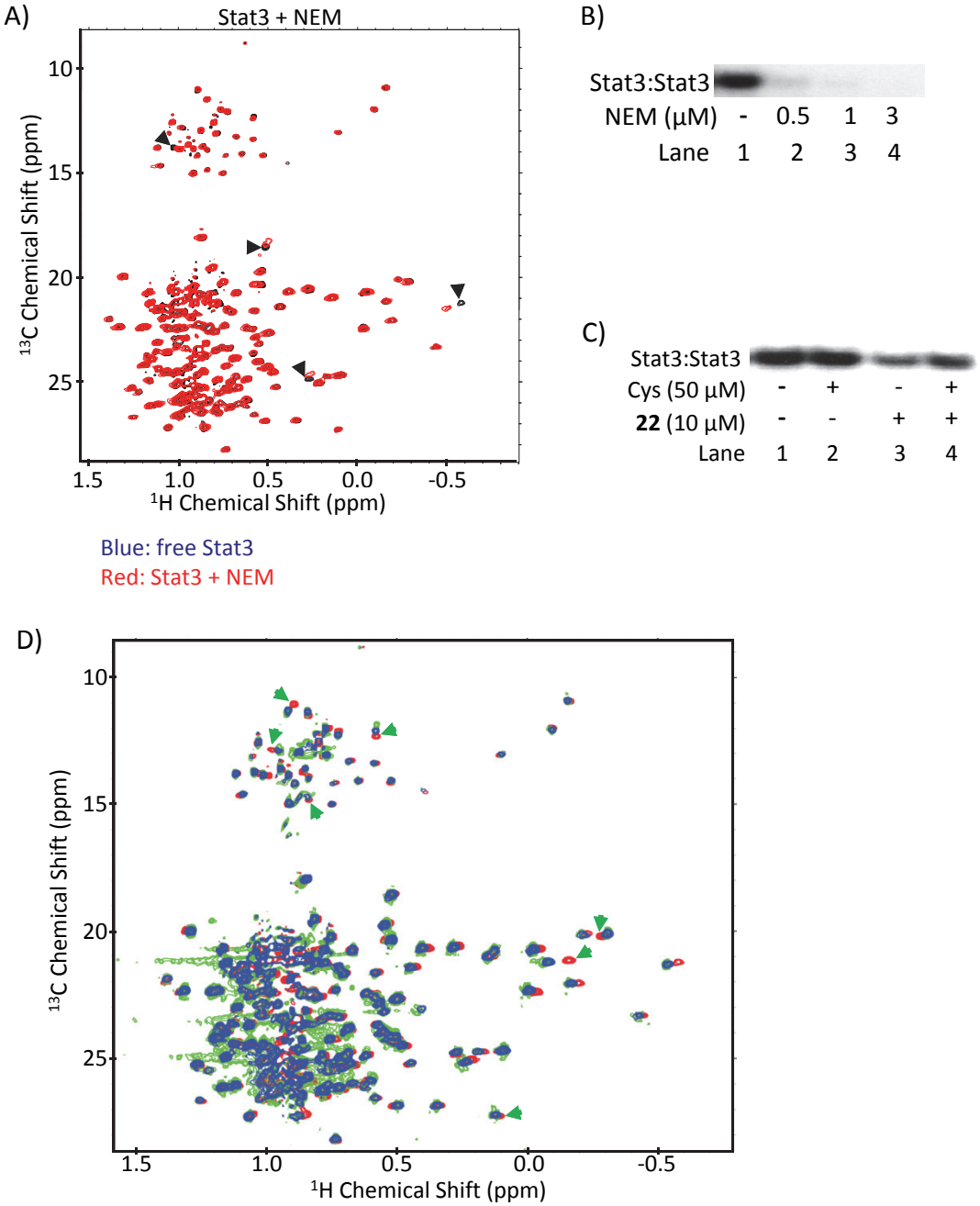
A)
Stat3 + NEM
10
15
20
25
^{13}C Chemical Shift (ppm)
1.5
1.0
0.5
0.0
-0.5
^{1}H Chemical Shift (ppm)
Blue: free Stat3
Red: Stat3 + NEM
B)
Stat3:Stat3
NEM (μM) - 0.5 1 3
Lane 1 2 3 4
C)
Stat3:Stat3
Cys (50 μM) - + - +
22 (10 μM) - - + +
Lane 1 2 3 4
D)
10
15
20
25
^{13}C Chemical Shift (ppm)
1.5
1.0
0.5
0.0
-0.5
^{1}H Chemical Shift (ppm)
Red: Wild-type Stat3
Green: Stat3V375A
Blue: Stat3L378A

Figure S3. **NMR analysis of wild-type and mutated Stat3 in solution with or without NEM and Stat3 DNA-binding activity and the effects of NEM or 22 in the presence or absence of Cysteine.** (A) Overlay of the ^{1}H-^{13}C HMQC spectra of wild-type Stat3, free (black) or wild-type Stat3 in the presence of NEM (red) showing residues with significant changes in either resonance line-widths or NMR chemical shifts that are indicated by arrowheads; (B and C) Stat3 DNA-binding assay of nuclear extracts prepared from NIH3T3/v-Src fibroblasts containing activated Stat3 pre-incubated for 30 min with (B) 0-3 μM NEM or (C) 10 μM **22** in the presence or absence of 50 μM cysteine (Cys) prior to incubation with the radiolabeled hSIE probe that binds Stat3 and subjecting to EMSA analysis; and (D) Overlay of the ^{1}H-^{13}C HMQC spectra of Stat3, wild-type (red) and mutant Stat3V375A (green) and Stat3L378A (blue). NEM-induced peak shifts or similar types are indicated by black arrowheads; peaks that are shifted and not due to treatment with NEM are indicated by green arrowheads. Positions of Stat3:DNA complex in gel are labeled; control lane (-) represents nuclear extracts pre-treated with 0.025% DMSO. Data are representative of 2-3 independent determinations.

Fig. S4

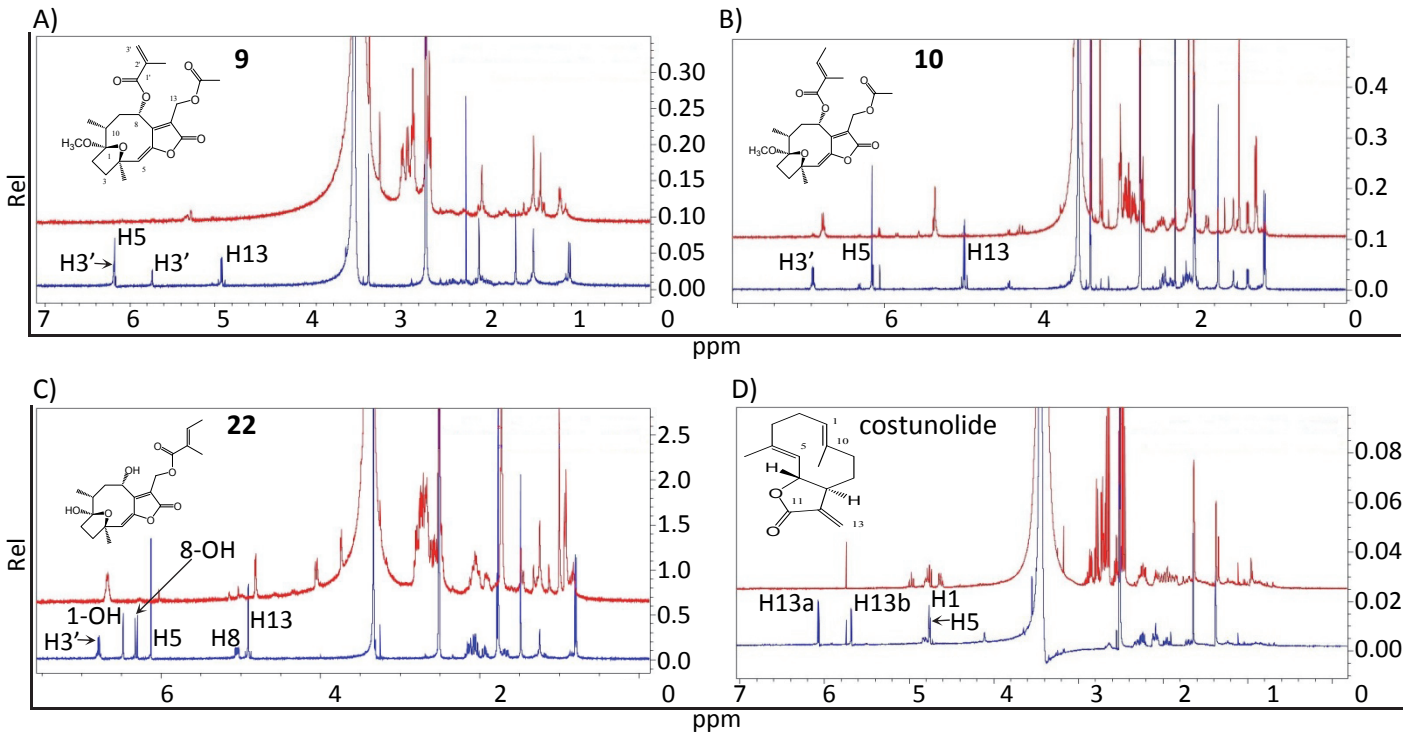

Blue: Compound alone

Red: Compound + 2 molar equivalent of cysteamine

Figure S4. ^{1}H NMR spectra of (A) **9**, (B) **10**, (C) **22** and (D) costunolide in DMSO-d_6 and the effects of the reactions with cysteamine (red) compared to compound alone control (blue). Data are representative of 2 independent determinations.

Fig. S5.

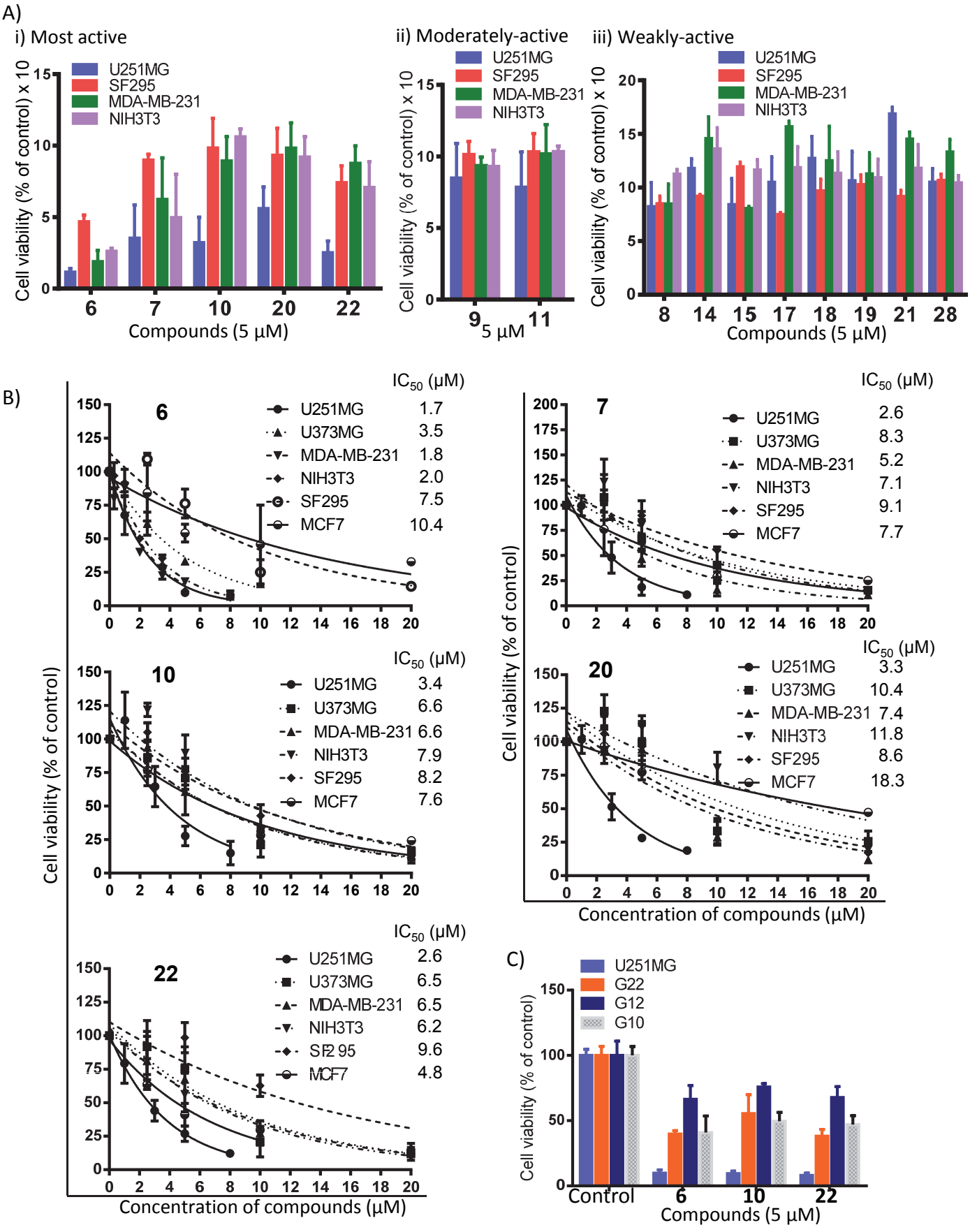
A)
i) Most active
ii) Moderately-active
iii) Weakly-active
U251MG
SF295
MDA-MB-231
NIH3T3
Cell viability (% of control) x 10
Compounds (5 µM)
B)
IC50 (µM)
6
U251MG 1.7
U373MG 3.5
MDA-MB-231 1.8
NIH3T3 2.0
SF295 7.5
MCF7 10.4
7
U251MG 2.6
U373MG 8.3
MDA-MB-231 5.2
NIH3T3 7.1
SF295 9.1
MCF7 7.7
10
U251MG 3.4
U373MG 6.6
MDA-MB-231 6.6
NIH3T3 7.9
SF295 8.2
MCF7 7.6
20
U251MG 3.3
U373MG 10.4
MDA-MB-231 7.4
NIH3T3 11.8
SF295 8.6
MCF7 18.3
22
U251MG 2.6
U373MG 6.5
MDA-MB-231 6.5
NIH3T3 6.2
SF295 9.6
MCF7 4.8
Cell viability (% of control)
Concentration of compounds (µM)
C)
U251MG
G22
G12
G10
Control
Compounds (5 µM)

Fig. S5.

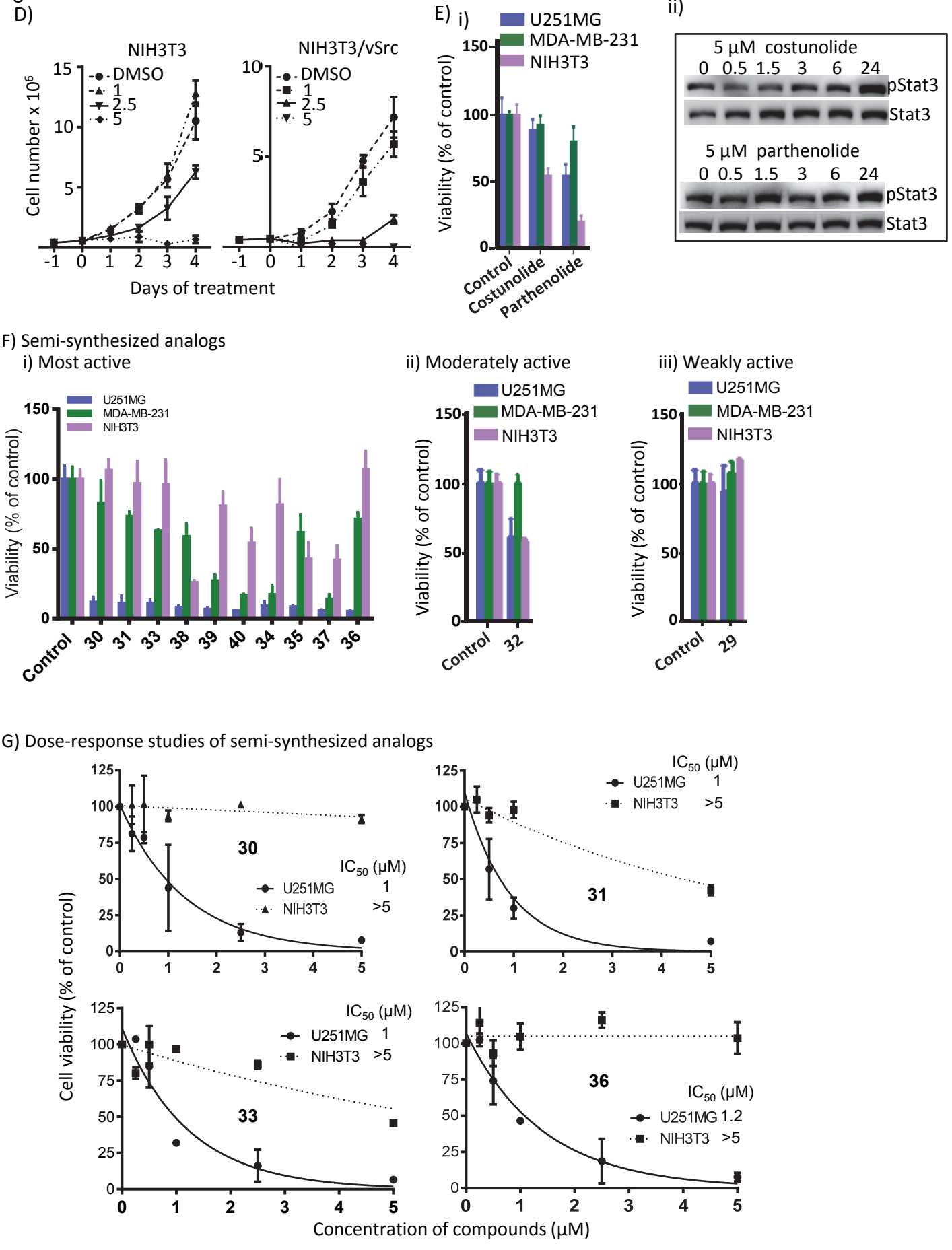
D)
NIH3T3
NIH3T3/vSrc
DMSO
1
2.5
5
Cell number x 10^6
Days of treatment
E) i)
U251MG
MDA-MB-231
NIH3T3
Viability (% of control)
Control
Costunolide
Parthenolide
ii)
5 μM costunolide
0 0.5 1.5 3 6 24
pStat3
Stat3
5 μM parthenolide
0 0.5 1.5 3 6 24
pStat3
Stat3
F) Semi-synthesized analogs
i) Most active
ii) Moderately active
iii) Weakly active
Control
30
31
33
38
39
40
34
35
37
36
32
29
G) Dose-response studies of semi-synthesized analogs
Cell viability (% of control)
IC50 (μM)
U251MG
NIH3T3
30
31
33
36
Concentration of compounds (μM)

Fig. S5.

H)

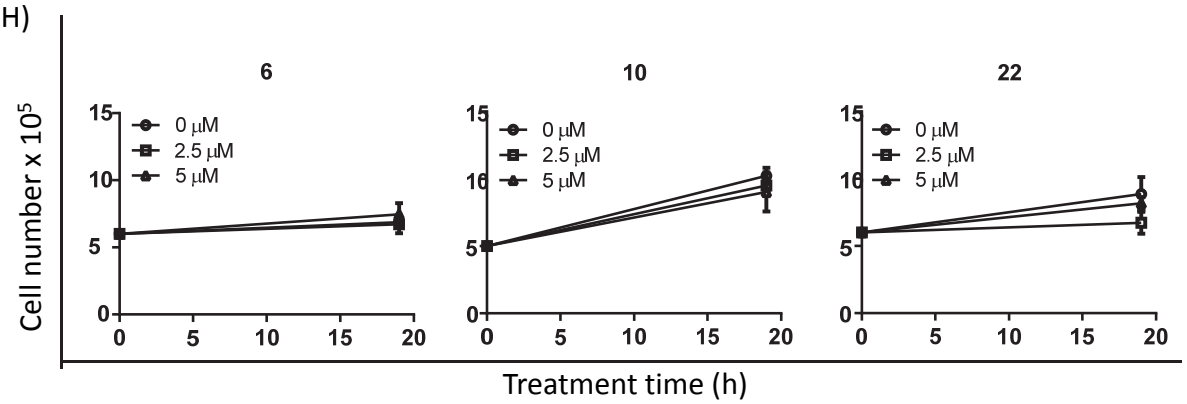
6
10
22
0 μM
2.5 μM
5 μM
Cell number x 10^5
Treatment time (h)

I)

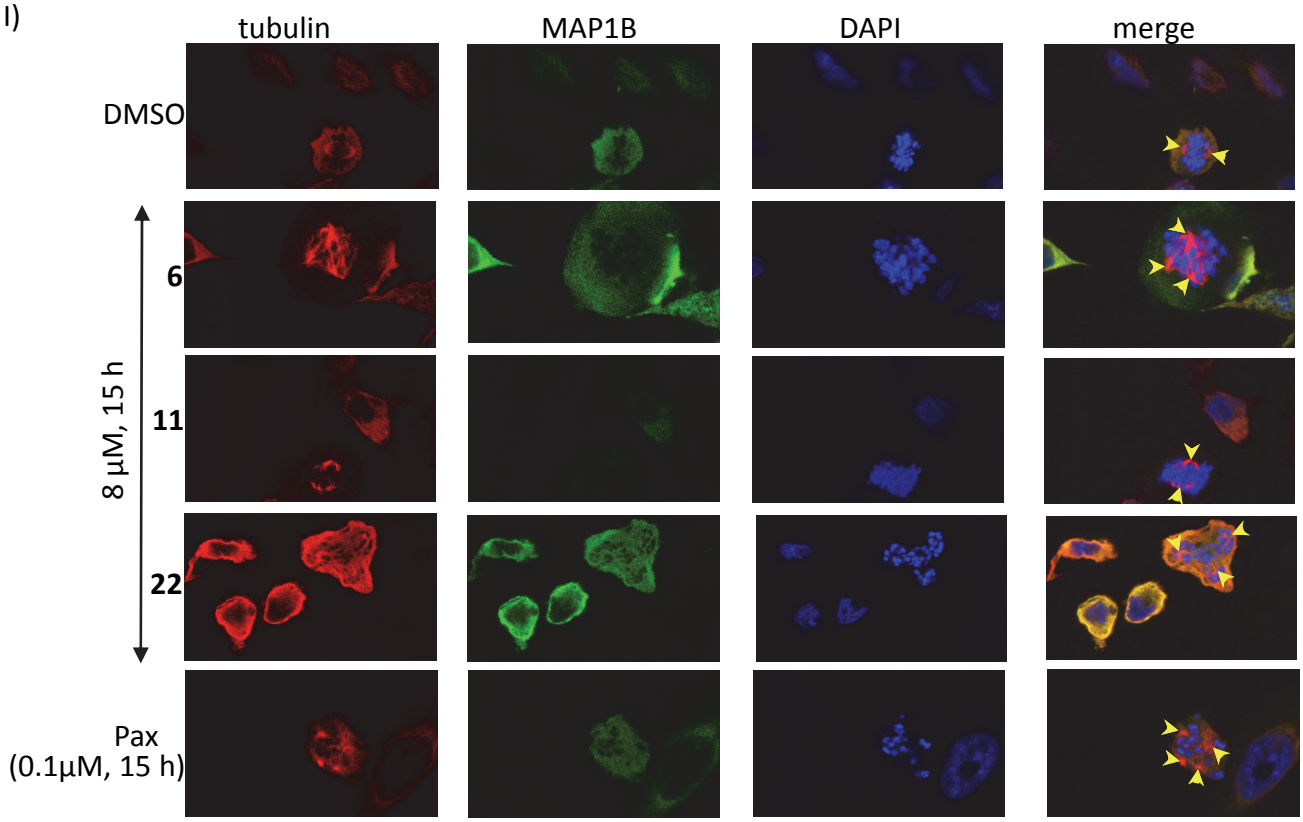
tubulin
MAP1B
DAPI
merge
DMSO
8 μM, 15 h
6
11
22
Pax
(0.1μM, 15 h)

Fig. S5.

J)

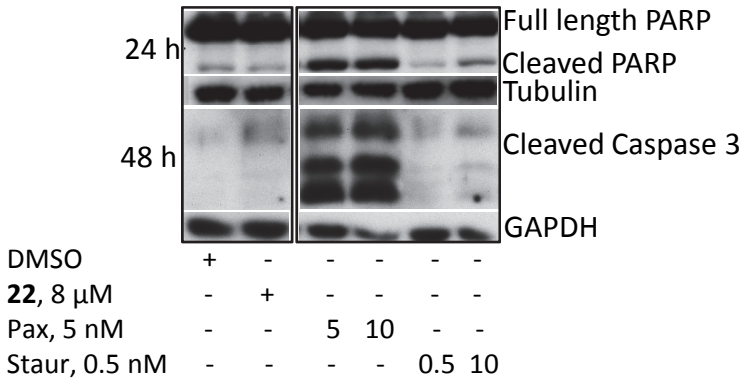
24 h
48 h
Full length PARP
Cleaved PARP
Tubulin
Cleaved Caspase 3
GAPDH
DMSO + - - - - -
22, 8 µM - + - - - -
Pax, 5 nM - - 5 10 - -
Staur, 0.5 nM - - - - 0.5 10

K)

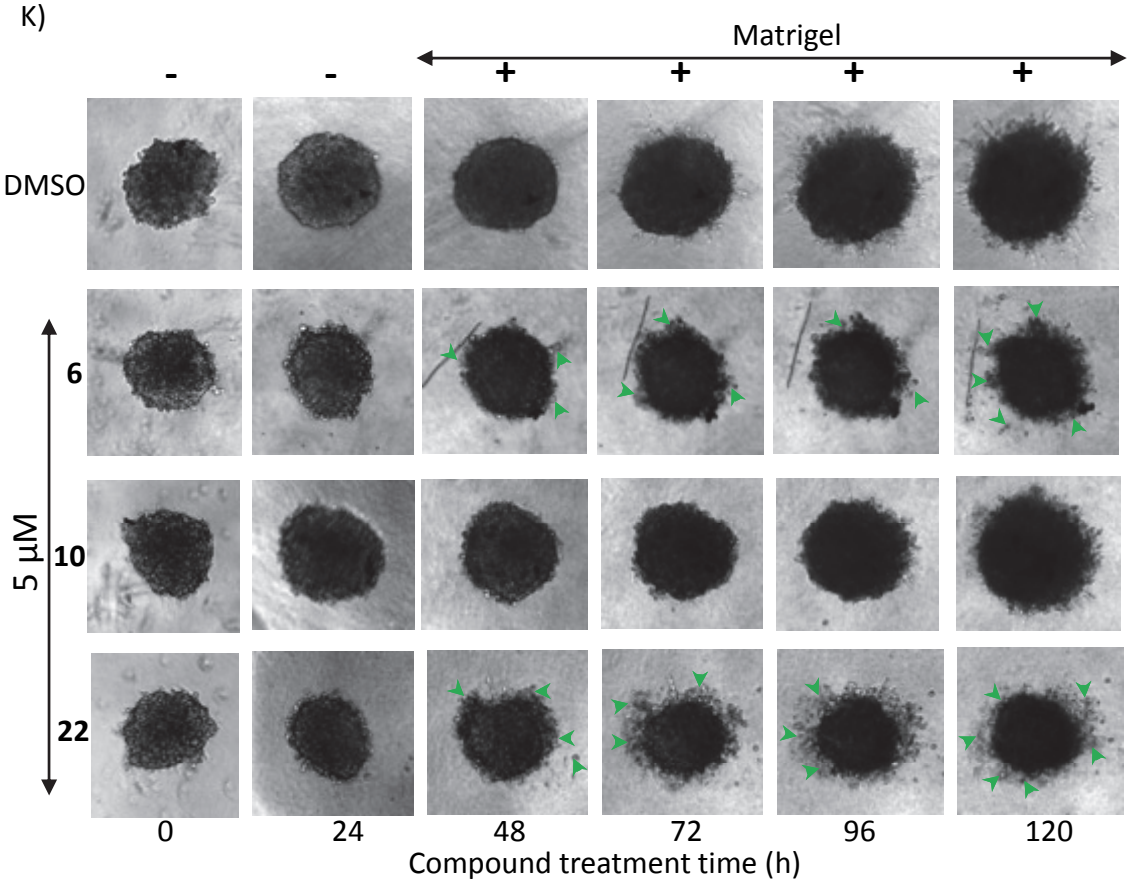
Matrigel
- - + + + +
DMSO
5 µM
6
10
22
0
24
48
72
96
120
Compound treatment time (h)

Figure S5. **Effects of hirsutinolides or semi-synthetic analogs on growth and viability of glioma cells in culture and as 3D spheroids.** (A-C) Cell viability plots for the effects on (A and B) human tumor or mouse cell lines and (C) patient-derived xenograft cells, G22 of 72-h treatments with (A) the designated hirsutinolides at 5 μM, (B) 0-20 μM **6**, **7**, **10**, **20** or **22**, and (C) 5 μM **6**, **10** or **22**. Insert, IC_{50} values determined from the dose-response curves; (D) Trypan blue exclusion/phase contrast microscopy for viable cell numbers and the effect of treatment with 0-5 μM **22** over four days; (E) Effect of 5 μM costunolide or parthenolide on the (i) viability of the indicated cell lines following 72-h treatment, or (ii) pStat3 and Stat3 levels, measured by immunoblotting analysis of whole-cell lysates from U251MG cells following 0-24 h treatment; (E and F) Cell viability plots for the effects of 72-h treatments with (F) 5 μM of the designated analogs on the indicated human tumor or mouse cell lines, and (G) 0-5 μM of the designated analogs on U251MG cells. Insert, IC_{50} values determined from the dose-response curves; (H) U251MG cells in culture were treated once with 0-5 μM **6**, **10** or **22** and viable cell numbers at 19 h post-treatment were counted and plotted; (I) U251MG cells growing on glass cover slips were synchronized by double thymidine block, released, and treated or untreated with the designated compounds for 15 h and processed for confocal microscopy imaging analysis of ß-tubulin, MAP1B, and DAPI using a Leica TCS SP5 confocal microscope. Images were captured and processed using LAS AF Lite software; Yellow arrowheads indicate poles; (J) Immunoblots of poly ADP ribose polymerase (PARP), caspase, tubulin and GAPDH and the effects of treatment with **22**, paclitaxel (Pax), and staurosporine (Staur) at the designated concentrations for 24 or 48 h; and (K) Human glioma patient-derived xenograft cells, G22 growing as 3D spheroids formed over a 48-h duration, were untreated (DMSO) or treated once with 5 μM **6**, **10** or **22** for 24 h prior to (-) the addition of matrigel (+), and allowed to grow for up to 120 h and imaged at 24 h intervals, which are shown. Green arrowheads indicate areas of extensive disaggregation. Positions of proteins in gel are labeled; control lane (-, 0) represents whole-cell lysates or cells treated with 0.025% DMSO. Data are representative of 2-4 independent determinations. Values are the mean ± S.D, n=3-4.

Fig. S6.

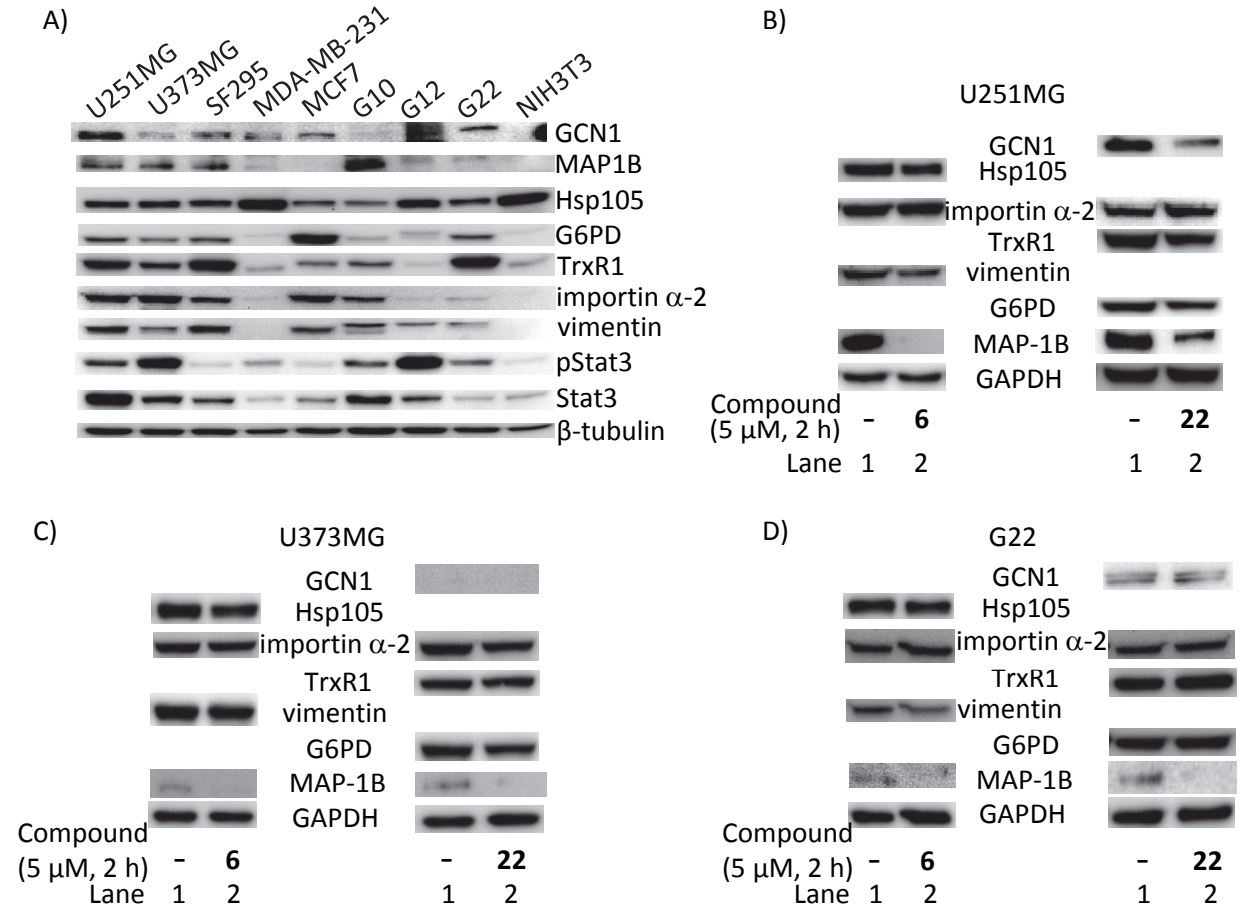
A)
U251MG
U373MG
SF295
MDA-MB-231
MCF7
G10
G12
G22
NIH3T3
GCN1
MAP1B
Hsp105
G6PD
TrxR1
importin α-2
vimentin
pStat3
Stat3
β-tubulin
B)
U251MG
GCN1
Hsp105
importin α-2
TrxR1
vimentin
G6PD
MAP-1B
GAPDH
Compound
(5 μM, 2 h)
- 6 - 22
Lane 1 2 1 2
C)
U373MG
GCN1
Hsp105
importin α-2
TrxR1
vimentin
G6PD
MAP-1B
GAPDH
Compound
(5 μM, 2 h)
- 6 - 22
Lane 1 2 1 2
D)
G22
GCN1
Hsp105
importin α-2
TrxR1
vimentin
G6PD
MAP-1B
GAPDH
Compound
(5 μM, 2 h)
- 6 - 22
Lane 1 2 1 2

Figure S6. **Hirsutinolides modulate GCN1, Hsp105, importin α-2, vimentin, G6PD, TrxR1 or MAP1B protein expression.** (A-D) Hsp105, importin subunit α-2, vimentin, TrxR1, GCN1, G6PD, MAP1B, GAPDH, and β-tubulin immunoblots in whole-cell lysates from the designated cell lines and patient-derived xenograft cells (A) untreated or (B-D) treated with 5 μM **6** or **22** for 2 h. Positions of proteins in gel are labeled; control lane (-) represents whole-cell lysates prepared from 0.025% DMSO-treated cells. Data are representative of 3 independent determinations.

Fig. S7.

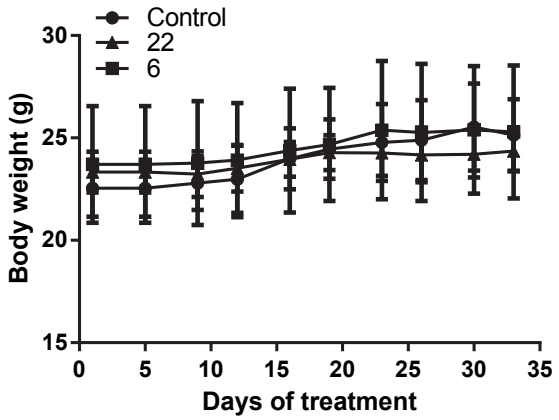
Control
22
6
Body weight (g)
30
25
20
15
0
5
10
15
20
25
30
35
Days of treatment

Figure S7. **Body weights of tumor-bearing mice treated with hirsutinolides.** Plots of body weight against days of treatment for mice bearing human glioma (U251MG) tumors and treated with **6** or **22** via oral gavage, 2 mg/kg or vehicle (1% DMSO) every other day for the indicated times. Body weights of mice were measured every 3-4 days and plotted.